
Sparse Bayesian Optimization

Sulin Liu^{*,1}

Qing Feng^{*,2}

David Eriksson^{*,2}

Benjamin Letham²

Eytan Bakshy²

¹Princeton University

²Meta

Abstract

Bayesian optimization (BO) is a powerful approach to sample-efficient optimization of black-box objective functions. However, the application of BO to areas such as recommendation systems often requires taking the interpretability and simplicity of the configurations into consideration, a setting that has not been previously studied in the BO literature. To make BO applicable in this setting, we present several regularization-based approaches that allow us to discover sparse and more interpretable configurations. We propose a novel differentiable relaxation based on homotopy continuation that makes it possible to target sparsity by working directly with L_0 regularization. We identify failure modes for regularized BO and develop a hyperparameter-free method, sparsity exploring Bayesian optimization (SEBO) that seeks to simultaneously maximize a target objective and sparsity. SEBO and methods based on fixed regularization are evaluated on synthetic and real-world problems, and we show that we are able to efficiently optimize for sparsity.

1 INTRODUCTION

Bayesian optimization (BO) is a technique for efficient global optimization that is used for parameter optimization across a wide range of applications, including robotics [Lizotte et al., 2007, Calandra et al., 2015], machine learning pipelines [Hutter et al., 2011, Snoek et al., 2012, Turner et al., 2021], internet systems [Letham et al., 2019, Feng et al., 2020], and chemistry [Gómez-Bombarelli et al., 2018, Felton et al., 2021]. In many applications, including those just mentioned, it is preferable for the optimized parameters to be sparse. One reason to prefer sparsity is that it increases

interpretability, a consideration that has recently attracted a great deal of attention in machine learning [Doshi-Velez and Kim, 2017, Rudin et al., 2022]. Interpretability is necessary for humans to be able to understand and evaluate the outputs of complex systems—the types of systems to which BO is often applied. In policy optimization, sparsity of the control policy provides a natural way for human decision-makers to gain insight into the behavior of the system, and identify potential issues [Ustun and Rudin, 2016, Hu et al., 2019]. Besides interpretability, sparsity can also be beneficial by producing systems that are easier to deploy and maintain, reducing the “tech debt” of machine learning systems [Sculley et al., 2015]. In chemistry, a sparse solution may require fewer reagents and steps to synthesize a compound.

Sparsity in machine learning is often achieved via regularization, such as L_1 regularization used by the lasso [Tibshirani, 1996], the group norm penalty used by the group lasso [Yuan and Lin, 2006], and L_0 regularization which directly targets setting elements to zero [Zhang, 2008]. The purpose of regularization in machine learning is typically to improve accuracy by reducing generalization error [Evgeniou et al., 2002]. In our setting, sparsity is a separate goal; interpretable sparse configurations will generally not improve the optimization objective, and in fact, may come at some cost to other metrics of system performance. Identifying such trade-offs is a central aspect of this work.

Sparsity in BO is an important topic that has not yet been addressed in the literature. Past work has used regularization in acquisition function optimization or modeling, but not for the purpose of sparsity in design parameters (see Section 2 for a review). Our work provides a thorough and broad treatment of sparsity in BO that fills in this gap. The main contributions of this paper are:

1. We study different approaches for incorporating sparse regularization into BO, and provide negative theoretical results showing that naïve forms of regularization can fail to optimize for certain levels of sparsity, regardless of the regularization coefficient.

^{*}Equal contribution

2. We draw connections between multi-objective BO and acquisition regularization, and show how multi-objective BO can be used for automatic selection of the regularization coefficient. We refer to this multi-objective formulation as the SEBO ("Sparsity Exploring Bayesian Optimization") method.
3. We develop a novel relaxation strategy for optimizing directly for L_0 sparsity, and show that it significantly outperforms the typical L_1 penalty.
4. We show that combining acquisition function regularization with sparse Gaussian process priors enables sparse optimization in high-dimensional spaces.
5. We provide the first results on achieving sparsity via BO, in a range of synthetic functions and on three real-world tasks (in systems configuration and AutoML). We also show the breadth of our method by using it to achieve different forms of sparsity such as feature-level and group sparsity.

Software for the methods developed in this paper is available at <http://to-be-released>.

Section 2 describes the necessary background and related work. Section 3 describes two natural approaches for incorporating sparse regularization into acquisition function optimization, both of which can fail to optimize for some levels of sparsity. Section 4 discusses a relationship between sparse BO and multi-objective BO, and describes how we can use methods from multi-objective BO to simultaneously optimize for all levels of sparsity. We describe how we optimize with L_0 regularization in Section 5. We demonstrate the usefulness of our methods by applying them to a set of synthetic and real-world benchmarks in Section 6. Finally, we discuss the results in Section 7.

2 BACKGROUND AND RELATED WORK

Bayesian Optimization: Shahriari et al. [2015] provide a thorough review of BO. In short, the goal is to maximize a black-box function $f : \mathbb{R}^D \rightarrow \mathbb{R}$ over a compact set $\mathcal{B} \subset \mathbb{R}^D$. We will assume that f is continuous and bounded on this domain. For simplicity, we also assume that the domain is the unit hypercube $[0, 1]^D$. At each iteration of optimization, f is modeled with a Gaussian process (GP) given the function evaluations observed so far, producing the normally distributed posterior $f(\mathbf{x}) \sim \mathcal{N}(\mu(\mathbf{x}), \sigma^2(\mathbf{x}))$. The location of the next function evaluation is selected by maximizing an acquisition function $\alpha(\mathbf{x})$ that encodes the value of observing \mathbf{x} for the goal of maximizing f . Typical acquisition functions include the expected improvement [EI, Jones et al., 1998] and the upper confidence bound [UCB, Srinivas et al., 2010]. EI is given by

$$\alpha_{\text{EI}}(\mathbf{x}) = \mathbb{E}_f [(f(\mathbf{x}) - f(\mathbf{x}^*))_+], \quad (1)$$

where \mathbf{x}^* is the best point observed so far. EI has a well-known analytic form in terms of the marginal posterior mean and variance. UCB is similarly computed directly from the marginal posterior,

$$\alpha_{\text{UCB}}(\mathbf{x}) = \mu(\mathbf{x}) + \sqrt{\beta}\sigma(\mathbf{x}), \quad (2)$$

where β is a hyperparameter that controls the exploration-exploitation trade-off. More recently, information-theoretic acquisition functions have been developed [Henrandez-Lobato et al., 2014, Wang and Jegelka, 2017].

Regularization in BO: Regularization has been applied to acquisition function optimization, though not for the purpose of sparsity. Shahriari et al. [2016] used regularization for unbounded BO, in which there are no bounds on the search space. They applied a form of L_2 regularization to the EI target value that penalized sampling points far from the initial center of the search space. Gonzalez et al. [2016] used regularization for batch BO, where the penalty discouraged points from being chosen close to points that had already been selected for the batch. The penalty was a function of the L_2 distance to already-selected points, and was directly multiplied to the acquisition function (EI or UCB).

BO with Sparse Models: Eriksson and Jankowiak [2021] introduced the sparse axis-aligned subspaces (SAAS) function prior in which a structured sparse prior is induced over the inverse-squared kernel lengthscales $\{\rho_i\}_{i=1}^d$ to enable BO in high dimensions. The SAAS prior has the form $\tau \sim \mathcal{HC}(\alpha)$, $\rho_i \sim \mathcal{HC}(\tau)$ where \mathcal{HC} is the half-Cauchy distribution which concentrates at zero. The goal of the SAAS prior is to turn off unimportant parameters by shrinking ρ_i to zero, which avoids overfitting in high-dimensional spaces, thus enabling sample-efficient high-dimensional BO. The global shrinkage parameter τ controls the overall model sparsity: as more observations are made, τ can be pushed to larger values, allowing the level of sparsity to adapt to the data as needed.

While sparsity in the GP model is different from the sparsity we seek in this work, we will show that combining the SAAS model with acquisition regularization is highly effective for sparse high-dimensional BO. By enforcing additional regularization in the acquisition function, the parameters identified as unimportant will be set to their baseline values, generating simpler and more interpretable policies. Other work has studied feature sparsity in GP regression but without considering sparsity in optimization [Oh et al., 2019, Park et al., 2021].

Multi-Objective BO: Multi-objective BO is used when there are several (often competing) objectives f_1, \dots, f_m and we wish to recover the Pareto frontier of non-dominated configurations. A popular method in this setting is ParEGO, which applies the standard single-objective EI acquisition function to a random scalarization of the

objectives [Knowles, 2006]. Many types of scalarizations have been developed for transforming multi-objective optimization (MOO) problems into single-objective problems [Ehrgott, 2005]. Recent work on multi-objective BO has focused on developing acquisition functions that explicitly target increasing the hypervolume of the known Pareto frontier with respect to a pre-specified reference point. Acquisition functions in this class, such as Expected Hypervolume Improvement (EHVI), are considered state-of-the-art for multi-objective BO [Yang et al., 2019, Daulton et al., 2020, 2021].

3 REGULARIZATION IN ACQUISITION FUNCTIONS

3.1 EXTERNAL REGULARIZATION

Perhaps the most straightforward approach for adding regularization to acquisition optimization is simply to add a regularization penalty directly to the acquisition function. This parallels the approach taken in regression with techniques like ridge regression and the lasso. Given a penalty term $\xi(\mathbf{x})$, we then maximize

$$\alpha_{\text{ER}}(\mathbf{x}; \lambda) = \alpha(\mathbf{x}) - \lambda\xi(\mathbf{x}) \quad (3)$$

to select the next point for evaluation. We refer to this approach as *external regularization* (ER). The penalty may be an L_0 norm¹ to target feature-level sparsity, $\xi(\mathbf{x}) = \|\mathbf{x}\|_0$, or can be adjusted for different forms of sparsity such as group sparsity. The regularization coefficient λ must be set, just as in the classical regularized regression setting.

This formulation separates the explore/exploit value of a point, encoded in α , from its sparsity value, encoded in ξ . This can perform poorly, because there is necessarily interaction between these two notions of value. We now provide a negative result showing that external regularization cannot capture certain levels of sparsity.

For this result, we will assume that the penalty term has a strict global minimum:

Assumption 1. ξ has a strict global minimum on \mathcal{B} at \mathbf{x}^S .

The point \mathbf{x}^S is the point of maximum sparsity. For $\xi(\mathbf{x}) = \|\mathbf{x}\|_0$ and a search space that includes the origin, Assumption 1 holds with $\mathbf{x}^S = 0$.

Theorem 1. Suppose $\alpha(\mathbf{x}) = 0$ for every \mathbf{x} where $\xi(\mathbf{x}) \leq \theta$. Then, for any value of $\lambda > 0$, every maximizer of $\alpha^{\text{ext}}(\mathbf{x}; \lambda)$ will satisfy $\xi(\mathbf{x}) > \theta$, or will equal \mathbf{x}^S .

¹Note that even though $\|\mathbf{x}\|_0 := |\{j : x_j \neq 0\}|$ does not actually satisfy the axioms of a vector norm, it is often referred to as a norm in the sparse optimization community.

The proof is given in Section S1 in the supplementary material. This result shows that if the acquisition value is 0 whenever the sparsity penalty is below a certain level θ , external regularization will not be able to recover any points with sparsity penalty below that level, other than the trivial point of maximum sparsity. This situation can easily be encountered in practice when there is a trade-off between the objective function and the sparsity. Consider the EI acquisition function with external regularization:

$$\alpha_{\text{EI-ER}}(\mathbf{x}; \lambda) = \mathbb{E}_f [(f(\mathbf{x}) - f(\mathbf{x}^*))_+] - \lambda\xi(\mathbf{x}). \quad (4)$$

Once the GP is confident that sparse points have worse objective value than non-sparse points, sparse points will have acquisition value approximately 0, as their improvement is being evaluated with respect to a non-sparse incumbent best \mathbf{x}^* . By Theorem 1, sparse points will then not be selected by the regularized acquisition function, regardless of how λ is tuned. Increasing λ will change the maximum from a non-sparse point directly to the trivial solution of \mathbf{x}^S , skipping all levels of sparsity in between. There is nothing in (4) to enable the acquisition function to select sparse points that improve over other points with a similar level of sparsity, which is necessary to fully explore the sparsity vs. objective trade-off.

3.2 INTERNAL REGULARIZATION

An alternative approach for adding regularization to the acquisition optimization is to add it directly to the objective function. In this approach, instead of using the posterior of f to compute the acquisition function, we compute the acquisition for the posterior of a regularized function:

$$g(\mathbf{x}; \lambda) = f(\mathbf{x}) - \lambda\xi(\mathbf{x}). \quad (5)$$

We refer to this as *internal regularization* (IR). The goal of the acquisition function is then to maximize g , which can be made to have a sparse maximizer by appropriately setting λ . With internal regularization, EI becomes

$$\begin{aligned} \alpha_{\text{EI-IR}}(\mathbf{x}; \lambda) &= \mathbb{E}_f [(g(\mathbf{x}) - g(\mathbf{x}^*))_+] \\ &= \mathbb{E}_f [(f(\mathbf{x}) - f(\mathbf{x}^*) - \lambda(\xi(\mathbf{x}) - \xi(\mathbf{x}^*)))_+], \end{aligned} \quad (6)$$

where \mathbf{x}^* is now the incumbent-best of g , not of f .

The difference between external and internal regularization depends on the acquisition function. It is easy to see that for the UCB acquisition of (2), they are identical. For EI they are not, as seen by comparing (4) and (6). For EI, internal regularization avoids some of the issues of external regularization by incorporating sparsity directly into the assessment of improvement. In (6), improvement is measured both in terms of increase of objective and increase in sparsity, and it is measured with respect to an incumbent best that has incorporated the sparsity penalty.

However, internal regularization can also be incapable of recovering points at every level of sparsity, as we will show now. For this result, we are interested in the optimal objective value as a function of sparsity level:

$$h(\theta) = \max_{\mathbf{x} \in \mathcal{B}} f(\mathbf{x}) \text{ subject to } \xi(\mathbf{x}) = \theta. \quad (7)$$

A trade-off between sparsity and objective would result in $h(\theta)$ increasing with θ , though it need not be strictly increasing. We now give the negative result for internal regularization, which assumes that ξ is continuous and bounded. See the supplementary material for more details.

Theorem 2. *For any θ in the interior of an interval where h is strictly convex, there is no maximizer of (5) with $\xi(\mathbf{x}) = \theta$, for any $\lambda > 0$.*

This result shows that internal regularization can only hope to recover optimal points at all sparsity levels if h is concave on its entire domain. This is a strong condition, one unlikely to hold for the types of functions typically of interest in BO, even with simple regularizers. Note that this result is independent of the choice of λ and the acquisition function used. If the desired level of sparsity happens to lie within a region where h is strictly convex, internal regularization can be expected to fail to find the optimum. Fig. S1 in the supplement shows an illustration of this result, in a problem where h has a region of strict convexity.

We will see in the empirical results that internal regularization performs better than external regularization, though, consistent with Theorem 2, can fail to cover the entire objective vs. sparsity trade-off. For EI with internal regularization, the expectation in (6) no longer has the closed form of regular EI, however this acquisition function can easily be computed and optimized using Monte Carlo methods [Wilson et al., 2018, Balandat et al., 2020]. In this paper we focus on EI, but both forms of regularization can be applied to any acquisition function, including entropy search methods. In entropy search, the acquisition function evaluates points according to their information gain with respect to the current belief about the location or function value of the optimum. The information gain will thus depend on the level of sparsity in a similar way as with EI, and so external vs. internal regularization have similar considerations.

4 MULTI-OBJECTIVE OPTIMIZATION AND SPARSITY

There are two fundamental challenges with both of the regularization approaches developed in Section 3. The first is that they both have a regularization coefficient λ that must be set. In a regression setting, the regularization coefficient is usually set to maximize cross-validation accuracy through hyperparameter optimization, often using grid search or

BO [Snoek et al., 2012]. In sparse BO, if there is a known desired level of sparsity, λ can be swept in each iteration of optimization to find a value that produces candidates with the desired level of sparsity. This significantly increases the overhead of BO by requiring hyperparameter optimization as part of every acquisition optimization. Furthermore, in real applications the desired level of sparsity is typically not known *a priori*. When there is a trade-off between interpretability and system performance, the desired level of interpretability will depend on what that trade-off looks like. In practice, we thus wish to identify the best-achievable objective at any particular level of sparsity. The second challenge is that, per the results of Theorems 1 and 2, we may not be able to identify the entire objective vs. sparsity trade-off, no matter how λ is swept. Depending on the problem, it may be that the sparsity levels of interest cannot be explored via either regularization strategy. Both of these challenges can be addressed by viewing sparse BO from the lens of multi-objective BO.

4.1 SPARSE BO AS MULTI-OBJECTIVE BO

In this section we introduce the Sparsity Exploring Bayesian Optimization method (SEBO), which takes a multi-objective approach to sparse BO. There is an insightful and useful connection between internal regularization and the random scalarization methods used for MOO. As described in Section 2, ParEGO applies the EI acquisition function to a random scalarization of multiple objectives. This is similar to EI with internal regularization, when we consider f and $-\xi$ to each be objectives, and the scalarization to be a linear weighting with λ the weight. In fact, linear scalarizations are commonly used in MOO [Marler and Arora, 2010].

Casting sparse BO as MOO of the objective and sparsity has several advantages. It provides a solution for setting the regularization coefficient λ , since we can use methods from multi-objective BO to optimally balance improvements in f and ξ with the goal of exploring the Pareto frontier. Random sampling of λ produces a ParEGO-style strategy for sparse BO, but we can also use more powerful approaches such as EHVI to select points that maximize performance for all levels of sparsity, or equivalently, maximize sparsity for all levels of performance. The goal of multi-objective BO is to identify the optimum for every level of sparsity, which enables decision makers to make an informed trade-off between interpretability and other considerations of system performance.

MOO also inspires new forms of regularization that can avoid the issues of Theorems 1 and 2. The inability of linear scalarizations to capture the entire Pareto front is a well-known failure mode for MOO, which has inspired a large number of alternative scalarizations [Das and Dennis, 1997]. ParEGO uses an augmented Chebyshev scalarization [Bowman, 1976], which, when applied to sparse regularization of

acquisition functions, means maximizing

$$T(\mathbf{x}; \lambda) = C(f(\mathbf{x}) - \lambda\xi(\mathbf{x})) - \max(f^* - f(\mathbf{x}), \lambda(\xi(\mathbf{x}) - \xi(\mathbf{x}^S))),$$

where f^* is an estimate for the maximum of f and C is a constant, usually set to 0.05. Unlike g in (5), maximizers of T span the entire objective vs. sparsity trade-off [Knowles, 2006]. Using EI to optimize this regularized function with randomly sampled values of λ is equivalent to applying ParEGO to the objective and the (negative) sparsity penalty.

Building on this relationship, we can apply state-of-the-art multi-objective BO methods to sparse BO by treating objective and sparsity as competing objectives, and can thus explicitly optimize for the entire regularization path. In our experiments, we use the EHVI acquisition function. Here, the hypervolume improvement is defined with respect to a worst-case reference point $\mathbf{r} = [r_f, r_\xi]$, can be set to estimates for the minimum and maximum values of f and ξ respectively. Given a set of observations $X^{\text{obs}} = \{\mathbf{x}^1, \dots, \mathbf{x}^n\}$, the Pareto hypervolume of that set is defined as

$$V(X^{\text{obs}}) = \lambda_M \left(\bigcup_{i=1}^n ([r_f, r_\xi] \times [f(\mathbf{x}^i), \xi(\mathbf{x}^i)]) \right),$$

where λ_M denotes the Lebesgue measure. The expected hypervolume improvement is then computed as

$$\alpha_{\text{SEBO}}(\mathbf{x}) = \mathbb{E}_f [V(X^{\text{obs}} \cup \{\mathbf{x}\}) - V(X^{\text{obs}})]. \quad (8)$$

We call this acquisition function SEBO, and explore its performance in combination with the L_0 sparse regularization, described next. This acquisition function is hyperparameter-free, and, as we will see, is highly effective for sparse BO.

5 OPTIMIZING ACQUISITION FUNCTIONS WITH L_0 SPARSITY

Our primary focus is L_0 sparsity, which comes with the challenge that the L_0 norm is discontinuous which makes the resulting acquisition function challenging to optimize. We will rely on a differentiable relaxation of the L_0 norm, namely

$$\|\mathbf{x}\|_0 \approx D - \sum_{i=1}^D \varphi_a(\mathbf{x}_i), \quad (9)$$

where $\varphi_a(r) = \exp(-0.5(r/a)^2)$, $a > 0$, and $\mathbf{x} \in \mathbb{R}^D$. While it may be tempting to set a to a small value, e.g., $a = 10^{-3}$, and optimize the acquisition function directly, this will not work well as the gradient of the relaxation is (numerically) zero almost everywhere in the domain. On the other hand, setting a to a large value, e.g., $a = 1$, will result in a poor approximation of $\|\mathbf{x}\|_0$ and the generated candidate will likely not be sparse.

Our approach follows the idea of homotopy continuation, which has been successfully applied to, for instance, solving nonlinear systems of equations and numerical bifurcation analysis [Allgower and Georg, 2012]. The main idea is to define a homotopy $H(\mathbf{x}, a)$, where $H(\mathbf{x}, a_1)$ corresponds to a problem that is easy to solve and $H(\mathbf{x}, a_k)$ corresponds to the target problem. We optimize the acquisition function using the differentiable relaxation introduced in (9) by solving a sequence of optimization problems given a strictly decreasing sequence $\{a_i\}_{i=1}^k$ and a starting point $\mathbf{x}^{(0)}$.

In order to approach the solution to the target problem $H(\mathbf{x}, a_k)$, we gradually reduce a from a sufficiently large a_1 to small a_k by exploiting the fact that $H(\mathbf{x}, a_1)$ is easy to solve and that the solution for $a = a_i$ provides a good starting point for $a = a_{i+1}$. In particular, we start from $\mathbf{x}^{(0)}$ and optimize the acquisition function with $a = a_1$ to generate $\mathbf{x}^{(1)}$, then start from $\mathbf{x}^{(1)}$ and optimize the acquisition function with $a = a_2$ to generate $\mathbf{x}^{(2)}$, until we have obtained a final candidate $\mathbf{x}^{(k)}$ that corresponds to $a = a_k$. This idea is illustrated in Fig. 1.

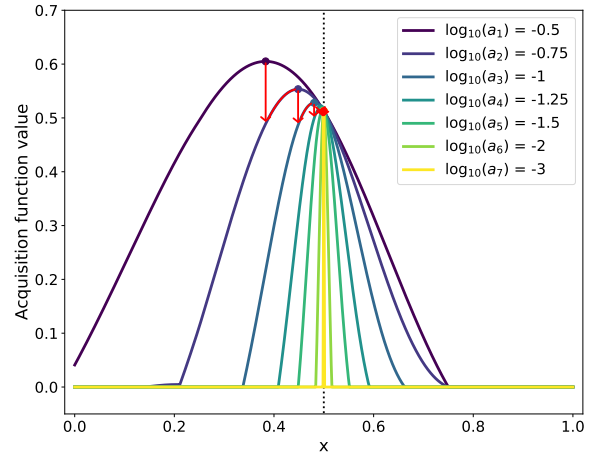


Figure 1: Consider the 1D problem of using SEBO to optimize $f(x) = -x^2$ with an L_0 penalty $\xi(x) = \|x - 0.5\|_0$. Assume $X^{\text{obs}} = \{0, 0.25, 0.75, 1.0\}$ have already been evaluated and we want to optimize SEBO to generate the next candidate. The global optimum of the acquisition function is given by the sparse point $x = 0.5$. We observe that the acquisition function is zero almost everywhere when $a = 10^{-3}$, but that optimizing the acquisition function for a decreasing sequence of a 's allows us to discover the global optimum of $x = 0.5$. The final configuration is shown as a red dot and the path is illustrated by red lines.

For all experiments in this paper, we use a sequence of 30 a 's starting from $10^{-0.5}$ and ending at 10^{-3} that is linearly spaced on a log-scale. We find $a_1 = 10^{-0.5}$ to be a robust choice that strikes a balance between being large enough to find initial points with non-zero acquisition function values, and being small enough to discover sparse points. To better understand this choice, note that

$\max_{x,z \in [0,1]} |\varphi'_{10-0.5}(x-z)| \approx 0.067$. On the other hand, $\max_{x,z \in [0,1]} |\varphi'_{10-1}(x-z)| \approx 2 \times 10^{-20}$, showing that $a = 0.1$ is too small to serve as the initial value of a .

6 EXPERIMENTS

We evaluate EI-IR, EI-ER and SEBO on two synthetic and three real-world problems. We show the results using L_0 regularization for most problems except for the last problem, where the group lasso is used to demonstrate that the methods can be applied to recover different forms of sparsity, such as group sparsity. In addition, we provide an ablation study that demonstrates the importance of using L_0 regularization by comparing it to L_1 regularization. We show in the ablation study that the homotopy continuation approach from Section 5 is crucial for effective L_0 regularization.

Experimental setup: Our experiments all have high-dimensional parameter spaces, so we use the SAAS model when optimizing with ER, IR, and SEBO. As baselines, we compare performance to quasi-random search (Sobol), BO with a standard ARD Matérn-5/2 kernel and the EI acquisition function (GPEI), and SAASBO. For the SAAS model, we use the same hyperparameters as suggested by Eriksson and Jankowiak [2021] and use the No-U-Turn sampler (NUTS) for model inference. The acquisition function is computed by averaging over the MCMC samples. We always scale the domain to be the unit hypercube $[0, 1]^D$ and standardize the objective to have mean 0 and variance 1 before fitting a GP. We use a deterministic model for the sparsity penalty when using it as an objective for SEBO. All figures show the mean results across replications (10 replications for the adaptive bitrate simulation (ABR) problem and 20 for all other experiments), and the error bars correspond to 2 standard errors. We assign replications an imputed function value in cases where a method is unable to find at least one configuration for a given level of sparsity. For all problems, this imputed value corresponds to the smallest label shown on the y-axis.

Synthetic functions: We first consider two synthetic problems where the level of sparsity is known. We use the Branin and Hartmann6 functions embedded into a 50D space, in which setting parameter values to 0 is considered sparse (so, typical L_0 sparsity), with negated function values to convert them to maximization problems. We used 50 trials (evaluations) with 8 quasi-random initial points for Branin and 100 trials with 20 quasi-random initial points for Hartmann6.

The results are shown in Fig. 2. The two leftmost plots show the optimization results by evaluating the objective only on observed points whose number of active (i.e., non-zero) parameters was less than or equal to the true effective dimension (2 for Branin and 6 for Hartmann6). We observe

that SEBO- L_0 performed the best, followed by IR with $\lambda = 0.001$. This suggests IR may perform competitively if the regularization coefficient is chosen optimally. On the other hand, ER performed worse than SEBO and IR. Finally, methods with non-regularized acquisition functions (Sobol, GPEI, and SAASBO) failed to identify sparse configurations. Fig. 2 (right) visualizes the trade-off between the objective and sparsity, in which SEBO- L_0 yielded the best sparsity trade-offs.

Ranking sourcing system simulation: The sourcing component of a recommendation system is responsible for retrieving a collection of items that are sent to the ranking algorithm for scoring. Items are retrieved from multiple sources, for instance that may represent different aspects of the user interest taxonomy [Wilhelm et al., 2018]. Querying for more items can potentially improve the quality of the recommendation system, but comes at the cost of increasing the infrastructure load. In addition, each source may require individual maintenance; thus, deprecating poor sources could reduce technical debt and maintenance costs of an entire recommendation system [Sculley et al., 2015]. Our goal is thus to identify a retrieval policy that uses a minimal number of sources while still maximizing the ranking quality score, measured by a function of content relevance and infrastructure load.

We developed a novel simulation of a recommender sourcing system that simulates the quality and infrastructure load of recommendations produced by a particular sourcing policy. The sourcing system is modeled as a topic model, where each source has a different distribution over topics, and topics have different levels of relevance to the user. When two sources are (topically) similar to one another, they may obtain duplicate items, which will not improve recommendation quality. Furthermore, each source has a cost associated with it, and retrieving more items from a source results in greater infrastructure load.

We consider a 25-dimensional retrieval policy in which each parameter specifies the number of items retrieved from a particular source. Our desired sparsity is thus to set parameters to 0, i.e., turning off the source. See Section S2.1 for more details. We used 8 initial points and ran 100 trials for all the methods. Fig. 3 (Left) shows that SEBO- L_0 performed the best in optimizing the ranking quality score under different sparsity levels. Sobol and GPEI could not find sparse policies and obtained worse quality scores even with 25 active parameters. IR and SAASBO performed similarly, and ER with the larger regularization parameter $\lambda = 0.01$ achieved higher quality score with less than 10 active dimensions.

SVM Machine learning hyperparameter tuning: We consider the problem of doing joint feature selection and hyperparameter tuning for a support vector machine (SVM). We tuned the C , ε , and γ hyperparameters of the SVM,

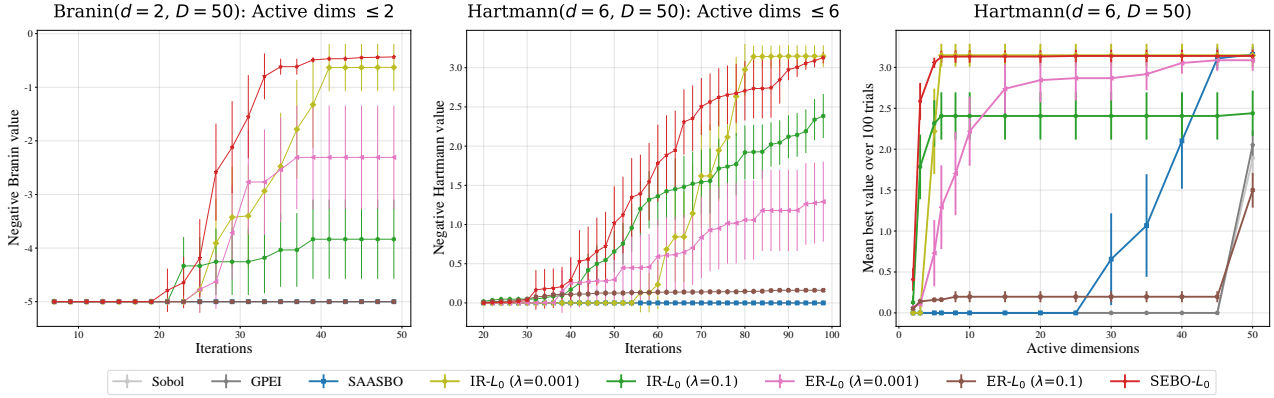


Figure 2: (Left) The best objective function value for Branin embedded into a 50D space, considering only observations with at most 2 active (non-sparse) parameters. SEBO- L_0 performed the best followed by IR with $\lambda = 0.001$. (Middle) SEBO- L_0 and IR with $\lambda = 0.001$ performed the best for the Hartmann6 function embedded into a 50D space when considering only observations with at most 6 active parameters. (Right) The objective-sparsity trade-off after all 100 iterations on the Hartmann6 problem. Shown is the best objective value found throughout the optimization when considering points with at most the specified number of active dimensions. SEBO- L_0 is able to effectively explore the entire trade-off between the objective and sparsity, and is able to discover sparse configurations with fewer than 6 active parameters that are not found by the other methods.

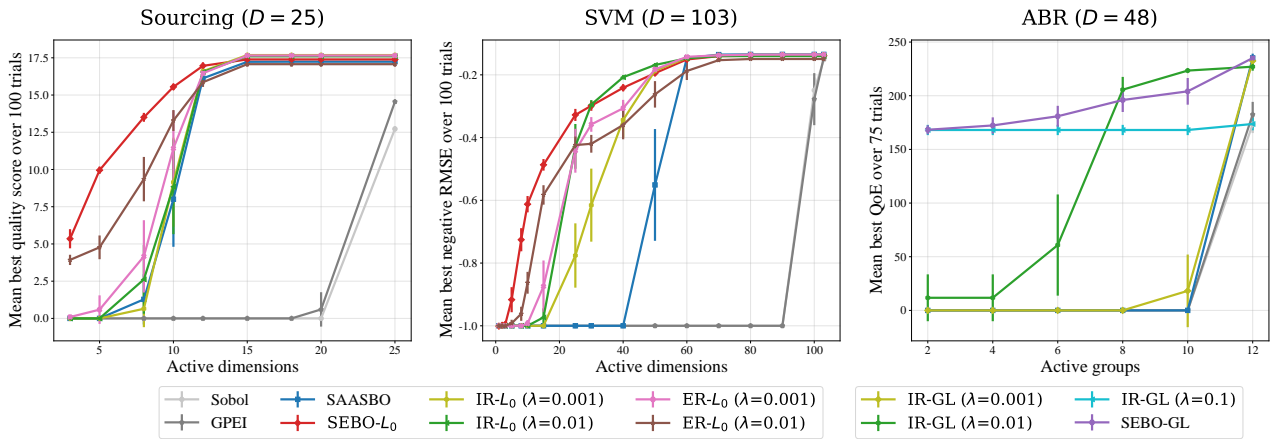


Figure 3: Objective-sparsity trade-offs after 100 (75 for ABR) trials for the three real-world problems. (Left) *Sourcing problem*: SEBO- L_0 regularization effectively explored all sparsity trade-offs. (Middle) *SVM problem*: ER with $\lambda = 0.01$ and IR with $\lambda = 0.01$ were able to explore parts of the Pareto frontier, however were dominated by SEBO- L_0 . (Right) *ABR problem*: Similar behavior as in the SVM problem was seen here with a group lasso penalty.

jointly with separate scale factors in the continuous range $[0, 1]$ for each feature. We used 100 features from the CT slice UCI dataset and the goal was to minimize the RMSE on the test set. This produces a 103D optimization problem where we shrink towards a scale factor of 0, as it effectively removes the feature from the dataset. We took $C \in [0.01, 1.0]$, $\varepsilon \in [0.01, 1.0]$, and $\gamma \in [0.001, 0.1]$, where the center of each interval was considered sparse as this is the default value in Sklearn. We optimized C , ε , γ on a log-scale, and initialized all methods with 20 points and ran 100 evaluations. Fig. 3 (Middle) shows that SEBO- L_0 was best able to explore the trade-offs between sparsity and (negative) RMSE.

Adaptive bitrate simulation: Video streaming and real-time conferencing systems use adaptive bitrate (ABR) algorithms to balance video quality and uninterrupted playback. The goal is to maximize the quality of experience (QoE). The optimal policy for a particular ABR controller may depend on the network, for instance a stream with large fluctuations in bandwidth will benefit from different ABR parameters than a stream with stable bandwidth. This motivates the use of a contextual policy where ABR parameters are personalized by context variables such as country or network type [Feng et al., 2020]. Various other systems and infrastructure applications commonly rely on tunable parameters which can benefit from contextualization.

We suppose that the system has already been optimized with a global non-contextual policy, π_{global} , that is used for all contexts. Our goal here is to use sparse BO to find the contextualized residuals $\Delta\pi_i$ for each individual context i , i.e., $\pi_i = \pi_{\text{global}} + \Delta\pi_i$. By regularizing the contextualized residuals $\Delta\pi_i$'s using the group lasso (GL) norm [Yuan and Lin, 2006], we hope to find policies that require minimum alteration to the global policy π_{global} , in which the minimum number of contexts have parameters that deviate from the global optimum. This adds both simplicity and interpretability to the contextual policy, since we can interpret the policy by looking at the contextual residuals $\Delta\pi_i$.

Fig. 3 (Right) shows the results of applying our methods to the contextual ABR optimization problem from Feng et al. [2020]. For this problem, we have 12 contexts and 4 parameters for each context resulting in a 48D optimization problem. We used 75 trials with 8 quasi-random initial points for all the methods. The group lasso penalty is defined by assigning parameters for each individual context to be within the same group. We observe that IR with a fixed λ was able to explore trade-offs at certain sparsity levels and that stronger regularization (larger λ) resulted in finding configurations that were more sparse. SEBO-GL, on the other hand, automatically and efficiently explored the trade-off between sparsity and reward at all sparsity levels. All other baselines (Sobol, GPEI, SAASBO) failed to find any sparse configurations that achieve non-zero reward.

Ablation study: We show by means of an ablation study the importance of using the homotopy continuation approach from Section 5 to target L_0 sparsity. We focus on SEBO as it consistently outperformed IR and ER, and refer to Fig. S5 in the supplementary material for additional results on the importance of using the SAAS model. The results from the ablation study can be seen in Fig. 4. Using a fixed value of a for the L_0 approximation performs poorly, particularly when a is small, which is due to the acquisition function being zero almost everywhere and thus difficult to optimize. On the other hand, $a = 1$ results in a failure to discover sparse configurations and the resulting method performs similar to SAASBO (see Fig. 2).

In addition, we show that for all approaches (ER, IR, and SEBO), working directly with L_0 regularization works significantly better than the frequently used L_1 regularization. This is consistent with recent work such as Zhang [2008], who state: ‘‘Despite of its success, L_1 regularization often leads to sub-optimal solutions because it is not a good approximation to L_0 regularization’’.

7 DISCUSSION

We have explored several approaches for achieving sparsity in BO. We compared the use of L_0 and L_1 regularization and concluded that L_0 regularization works significantly better. However, as the L_0 norm is not even continuous,

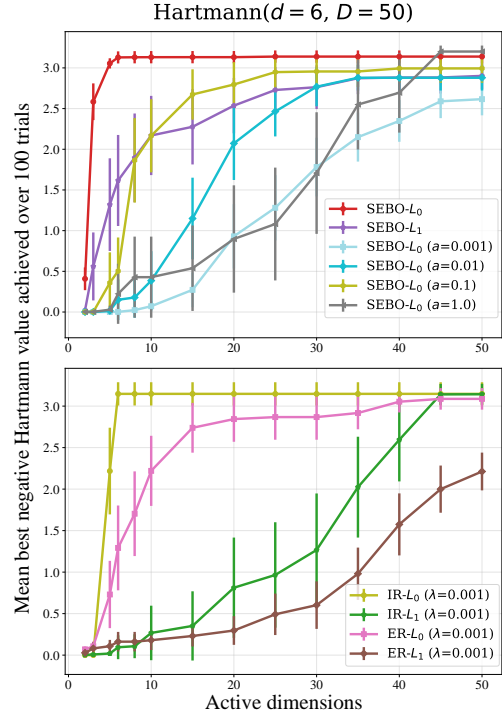


Figure 4: Ablation study on the Hartmann6 function embedded in a 50D space. (Upper) SEBO- L_0 works much better than SEBO- L_1 as it directly targets sparsity. Using a fixed value of a performs poorly, confirming the importance of our homotopy continuation approach. (Lower) Working directly with L_0 regularization works drastically better than L_1 regularization for both IR and ER.

this required developing a novel approach for optimizing the acquisition function using homotopy continuation. We observed that external and internal regularization generally performed poorly, showing significant sensitivity to the value of the regularization coefficient. Setting the value of the regularization regularization coefficient is challenging as it is problem-dependent and setting it sub-optimally can significantly degrade the results. To combat this, we introduced the SEBO method which was motivated by the relationship between internal regularization and MOO. SEBO- L_0 consistently outperformed internal and external regularization and was able efficiently map out the entire objective vs. sparsity trade-off. Moreover, SEBO is hyperparameter-free and avoided the use of a tuned regularization coefficient. Finally, we showed that sparse BO is especially powerful when combined with the sparsity-inducing SAAS prior.

The methods we developed in this paper apply to a broad range of problems. We have demonstrated their usefulness on a wide range of problems with different types of sparsity, e.g., feature-level sparsity and group sparsity. We expect the insights developed in this paper to be useful in other areas of BO where regularization has previously been used, such as unbounded BO and batch BO.

REFERENCES

- E. L. Allgower and K. Georg. *Numerical continuation methods: an introduction*, volume 13. Springer Science & Business Media, 2012.
- M. Balandat, B. Karrer, D. R. Jiang, S. Daulton, B. Letham, A. G. Wilson, and E. Bakshy. BoTorch: A framework for efficient Monte-Carlo Bayesian optimization. In *Advances in Neural Information Processing Systems 33*, NeurIPS, 2020.
- D. M. Blei, A. Y. Ng, and M. I. Jordan. Latent dirichlet allocation. *Journal of machine Learning research*, 3(Jan): 993–1022, 2003.
- V. J. Bowman. On the relationship of the Tchebycheff norm and the efficient frontier of multiple-criteria objectives. In H. Thiriez and S. Zionts, editors, *Multiple Criteria Decision Making. Lecture Notes in Economics and Mathematical Systems (Operations Research)*, vol 130, pages 76–86. Springer Berlin, Heidelberg, 1976.
- R. Calandra, A. Seyfarth, J. Peters, and M. P. Deisenroth. Bayesian optimization for learning gaits under uncertainty. *Annals of Mathematics and Artificial Intelligence*, 76(1):5–23, 2015.
- I. Das and J. Dennis. A closer look at drawbacks of minimizing weighted sums of objectives for Pareto set generation in multicriteria optimization problems. *Structural Optimization*, 14:63–69, 1997.
- S. Daulton, M. Balandat, and E. Bakshy. Differentiable expected hypervolume improvement for parallel multi-objective Bayesian optimization. *Advances in Neural Information Processing Systems*, 33:9851–9864, 2020.
- S. Daulton, M. Balandat, and E. Bakshy. Parallel Bayesian optimization of multiple noisy objectives with expected hypervolume improvement. *Advances in Neural Information Processing Systems*, 34, 2021.
- F. Doshi-Velez and B. Kim. Towards a rigorous science of interpretable machine learning. *arXiv preprint arXiv:1702.08608*, 2017.
- M. Ehrgott. *Multicriteria Optimization*. Springer Berlin, Heidelberg, 2005.
- D. Eriksson and M. Jankowiak. High-dimensional Bayesian optimization with sparse axis-aligned subspaces. In *Proceedings of the 37th Conference on Uncertainty in Artificial Intelligence*, UAI, pages 493–503, 2021.
- T. Evgeniou, T. Poggio, M. Pontil, and A. Verri. Regularization and statistical learning theory for data analysis. *Computational Statistics & Data*, 38(4):421–432, 2002.
- K. Felton, J. Rittig, and A. Lapkin. Summit: Benchmarking machine learning methods for reaction optimisation. *Chemistry Methods*, 1(2):116–122, 2021.
- Q. Feng, B. Letham, H. Mao, and E. Bakshy. High-dimensional contextual policy search with unknown context rewards using Bayesian optimization. In *Advances in Neural Information Processing Systems 33*, NeurIPS, pages 22032–22044, 2020.
- R. Gómez-Bombarelli, J. N. Wei, D. Duvenaud, J. M. Hernández-Lobato, B. Sánchez-Lengeling, D. Sheberla, J. Aguilera-Iparraguirre, T. D. Hirzel, R. P. Adams, and A. Aspuru-Guzik. Automatic chemical design using a data-driven continuous representation of molecules. *ACS Central Science*, 4(2):268–276, 2018.
- J. González, Z. Dai, P. Hennig, and N. Lawrence. Batch Bayesian optimization via local penalization. In *Proceedings of the 19th International Conference on Artificial Intelligence and Statistics*, AISTATS, pages 648–657, 2016.
- J. M. Hernández-Lobato, M. W. Hoffman, and Z. Ghahramani. Predictive entropy search for efficient global optimization of black-box functions. In *Advances in Neural Information Processing Systems 27*, NIPS, pages 918–926, 2014.
- X. Hu, C. Rudin, and M. Seltzer. Optimal sparse decision trees. In *Advances in Neural Information Processing Systems 32*, NeurIPS, pages 7267–7275, 2019.
- F. Hutter, H. H. Hoos, and K. Leyton-Brown. Sequential model-based optimization for general algorithm configuration. In *International Conference on Learning and Intelligent Optimization*, LION, pages 507–523, 2011.
- D. R. Jones, M. Schonlau, and W. J. Welch. Efficient global optimization of expensive black-box functions. *Journal of Global Optimization*, 13:455–492, 1998.
- J. Knowles. ParEGO: A hybrid algorithm with on-line landscape approximation for expensive multiobjective optimization problems. *IEEE Transactions on Evolutionary Computation*, 10(1):50–66, 2006.
- B. Letham, B. Karrer, G. Ottoni, and E. Bakshy. Constrained Bayesian optimization with noisy experiments. *Bayesian Analysis*, 14(2):495–519, 2019.
- D. J. Lizotte, T. Wang, M. Bowling, and D. Schuurmans. Automatic Gait Optimization with Gaussian Process Regression. In *Proceedings of the 20th International Joint Conference on Artificial Intelligence*, IJCAI, pages 944–949, 2007.
- R. T. Marler and J. S. Arora. The weighted sum method for multi-objective optimization: New insights. *Structural and Multidisciplinary Optimization*, 41:853–862, 2010.

- C. Oh, J. M. Tomczak, E. Gavves, and M. Welling. Combinatorial Bayesian optimization using the graph Cartesian product. In *Advances in Neural Information Processing Systems 32*, NeurIPS, pages 2914–2924, 2019.
- C. Park, D. J. Borth, N. S. Wilson, and C. N. Hunter. Variable selection for Gaussian process regression through a sparse projection. *IJSE Transactions*, pages 1–14, 2021.
- C. Rudin, C. Chen, Z. Chen, H. Huang, L. Semenova, and C. Zhong. Interpretable machine learning: Fundamental principles and 10 grand challenges. *Statistics Surveys*, 16: 1–85, 2022.
- D. Sculley, G. Holt, D. Golovin, E. Davydov, T. Phillips, D. Ebner, V. Chaudhary, M. Young, J.-F. Crespo, and D. Dennison. Hidden technical debt in machine learning systems. In *Advances in Neural Information Processing Systems 28*, NIPS, pages 2503–2511, 2015.
- B. Shahriari, K. Swersky, Z. Wang, R. P. Adams, and N. de Freitas. Taking the human out of the loop: A review of Bayesian optimization. *Proceedings of the IEEE*, 104(1):148–175, 2015.
- B. Shahriari, A. Bouchard-Côté, and N. de Freitas. Unbounded Bayesian optimization via regularization. In *Proceedings of the 19th International Conference on Artificial Intelligence and Statistics*, AISTATS, pages 1168–1176, 2016.
- J. Snoek, H. Larochelle, and R. P. Adams. Practical Bayesian optimization of machine learning algorithms. In *Advances in Neural Information Processing Systems 25*, NIPS, pages 2951–2959, 2012.
- N. Srinivas, A. Krause, S. Kakade, and M. Seeger. Gaussian process optimization in the bandit setting: No regret and experimental design. In *Proceedings of the 27th International Conference on Machine Learning*, ICML, pages 1015–1022, 2010.
- R. Tibshirani. Regression shrinkage and selection via the lasso. *Journal of the Royal Statistical Society: Series B*, 58(1):267–288, 1996.
- R. Turner, D. Eriksson, M. McCourt, J. Kiili, E. Laaksonen, Z. Xu, and I. Guyon. Bayesian optimization is superior to random search for machine learning hyperparameter tuning: Analysis of the black-box optimization challenge 2020. In *NeurIPS 2020 Competition and Demonstration Track*, pages 3–26, 2021.
- B. Ustun and C. Rudin. Supersparse linear integer models for optimized medical scoring systems. *Machine Learning*, 102(3):349–391, 2016.
- Z. Wang and S. Jegelka. Max-value entropy search for efficient Bayesian optimization. In *Proceedings of the 34th International Conference on Machine Learning*, ICML, pages 3627–3635, 2017.
- M. Wilhelm, A. Ramanathan, A. Bonomo, S. Jain, E. H. Chi, and J. Gillenwater. Practical diversified recommendations on youtube with determinantal point processes. In *Proceedings of the 27th ACM International Conference on Information and Knowledge Management*, CIKM '18, page 2165–2173, New York, NY, USA, 2018. Association for Computing Machinery. doi: 10.1145/3269206.3272018.
- J. Wilson, F. Hutter, and M. Deisenroth. Maximizing acquisition functions for Bayesian optimization. In *Advances in Neural Information Processing Systems 31*, NeurIPS, 2018.
- K. Yang, M. Emmerich, A. Deutz, and T. Bäck. Multi-objective Bayesian global optimization using expected hypervolume improvement gradient. *Swarm and Evolutionary Computation*, 44:945–956, 2019.
- M. Yuan and Y. Lin. Model selection and estimation in regression with grouped variables. *Journal of the Royal Statistical Society: Series B*, 68(1):49–67, 2006.
- T. Zhang. Multi-stage convex relaxation for learning with sparse regularization. *Advances in neural information processing systems*, 21, 2008.

S1 THEORETICAL RESULTS

Here we provide the proofs of Theorems 1 and 2, as well as an illustration of the result of 2.

Proof of Theorem 1. Suppose $\mathbf{x}^\dagger \in \arg \max \alpha^{\text{ext}}(\mathbf{x}; \lambda)$ and $\xi(\mathbf{x}^\dagger) \leq \theta$. Then, $\alpha(\mathbf{x}^\dagger) = 0$, so $\alpha^{\text{ext}}(\mathbf{x}^\dagger; \lambda) = -\lambda\xi(\mathbf{x}^\dagger)$.

By \mathbf{x}^\dagger being a maximizer of α^{ext} we must have

$$-\lambda\xi(\mathbf{x}^\dagger) = \alpha^{\text{ext}}(\mathbf{x}^\dagger; \lambda) \geq \alpha^{\text{ext}}(\mathbf{x}^S; \lambda) = -\lambda\xi(\mathbf{x}^S).$$

Thus $\xi(\mathbf{x}^\dagger) \leq \xi(\mathbf{x}^S)$. By Assumption 1, we have then that $\mathbf{x}^\dagger = \mathbf{x}^S$. \square

We assume ξ is continuous and bounded, which implies h is continuous and bounded:

Assumption 2. ξ is continuous on \mathcal{B} , and has minimum value $\xi(\mathbf{x}^S) = s_l$ and maximum value s_u .

Proposition 1. h is continuous and bounded on the domain $[s_l, s_u]$.

Sketch of Proof. This result falls from the continuity and boundedness of f , and by applying the intermediate value theorem to ξ . \square

Theorem 2 requires Assumption 2.

Proof of Theorem 2. Suppose h is strictly convex over the interval $[\theta_l, \theta_u]$. For the sake of contradiction, assume that there exists a $\theta_\dagger \in (\theta_l, \theta_u)$ and an \mathbf{x}^\dagger such that $\mathbf{x}^\dagger \in \arg \max g(\mathbf{x}; \lambda)$ and $\xi(\mathbf{x}^\dagger) = \theta_\dagger$.

It is clear that $\mathbf{x}^\dagger \in \arg \max f(\mathbf{x})$ subject to $\xi(\mathbf{x}) = \theta_\dagger$, otherwise the point with strictly larger f and equal ξ value would have a higher value for g , and \mathbf{x}^\dagger could not be optimal for g . Thus, $f(\mathbf{x}^\dagger) = h(\theta_\dagger)$.

We can express $\theta_\dagger = t\theta_l + (1-t)\theta_u$ for some $t \in (0, 1)$. By strict convexity of h on this interval, we have that

$$h(\theta_\dagger) < th(\theta_l) + (1-t)h(\theta_u). \quad (\text{S1})$$

Take $\mathbf{x}^u \in \arg \max f(\mathbf{x})$ subject to $\xi(\mathbf{x}) = \theta_u$, and $\mathbf{x}^l \in \arg \max f(\mathbf{x})$ subject to $\xi(\mathbf{x}) = \theta_l$. These are the points in \mathcal{B} corresponding to $h(\theta_l)$ and $h(\theta_u)$. The optimality of \mathbf{x}^\dagger implies that $g(\mathbf{x}^\dagger; \lambda) \geq g(\mathbf{x}^u; \lambda)$ and $g(\mathbf{x}^\dagger; \lambda) \geq g(\mathbf{x}^l; \lambda)$. Thus,

$$\begin{aligned} g(\mathbf{x}^\dagger; \lambda) &\geq tg(\mathbf{x}^l; \lambda) + (1-t)g(\mathbf{x}^u; \lambda) \\ h(\theta_\dagger) - \lambda\theta_\dagger &\geq th(\theta_l) - t\lambda\theta_l + (1-t)h(\theta_u) - (1-t)\lambda\theta_u \\ h(\theta_\dagger) &\geq th(\theta_l) + (1-t)h(\theta_u), \end{aligned} \quad (\text{S2})$$

using $\theta_\dagger = t\theta_l + (1-t)\theta_u$. The result in (S2) contradicts the convexity in (S1), and so \mathbf{x}^\dagger cannot be optimal for g . \square

Fig. S1 shows an illustration of the result of Theorem 2 on a log-transformed version of the classic Branin problem, where $f(x_1, x_2) = -\log(10 + \text{Branin}(x_1, x_2))$, and we are using a traditional L_1 regularization penalty, $\xi(x_1, x_2) = |x_1| + |x_2|$. The right panel shows $h(\theta)$, from (7), as it traces the trade-off from the minimum of ξ to the maximum of f . There is a wide interval of L_1 -norm values in the middle, 0.4 to 2.7, where $h(\theta)$ is strictly convex. By Theorem 2, there is no value of λ under which the maximizer of (5) has L_1 norm in that range. That range of sparsity levels thus cannot be reached by maximizing the regularized function g .

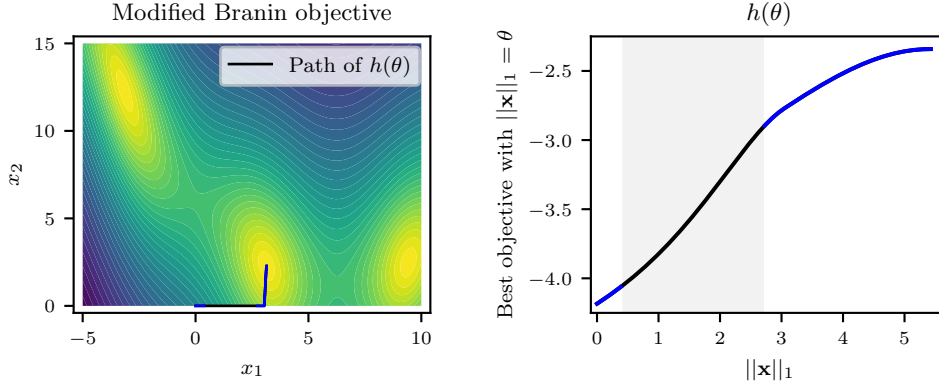


Figure S1: An illustration of the internal regularization result in Theorem 2. (Left) The objective f is a modified Branin function. The sparsity penalty ξ is the L_1 norm. (Right) The optimal objective vs. sparsity trade-off, $h(\theta)$, shows the best-achievable objective value for any specified value of L_1 norm. The shaded region is an interval where h is strictly convex. By Theorem 2, the regularized function in (5) has no maximizers with L_1 norm in that range, for any value of λ .

S2 ADDITIONAL EXPERIMENTAL STUDIES

S2.1 RANKING SOURCING SYSTEM SIMULATION

In the sourcing simulation experiment in Section 6, the recommender sourcing system has 25 content sources and 1000 possible pieces of content (i.e., *items*) for retrieval. We consider a 25-dimensional retrieval policy \mathbf{x} over the integer domain $[0, 50]^{25}$. We take inspiration from the Latent Dirichlet Allocation (LDA) model [Blei et al., 2003] in defining a generative probabilistic model of items recommended by each source. We assume there are 8 latent topics and that each item can be represented as a mixture over topics. Each source contains a mixture over a set of topics, and particular items will be more likely to be recommended by topically related sources. Such topical overlaps can create redundancy of recommendations across sources. Retrieving more items from additional sources comes at a cost making sparse retrieval policies preferred.

Before describing the simulation in pseudo-code, we need the following definitions:

- T is the number of latent topics.
- K is the number of distinct items.
- S is the number of content sources.
- $\theta_s \in \Delta^T$ is the topic distribution for source s , where Δ^T denotes the T -dimensional simplex. $\{\theta_s\}_{s=1}^S$ follow a Dirichlet distribution, i.e., $\theta_s \sim \text{Dir}(\alpha)$ where $\alpha = 0.2$.
- $\phi_i \in \Delta^K$ is the item distribution for each topic i , where Δ^K denotes the K -dimensional simplex. $\{\phi_i\}_{i=1}^T$ also follow a Dirichlet distribution, i.e., $\phi_i \sim \text{Dir}(\beta)$ where $\beta = 0.5$.
- $z_{s,k}$ is the topic assignment for item k in source s and follows multinomial distribution: $z_{s,k} \sim \text{Multi}(\theta_s)$
- $w_{s,k}$ is the indicator of item k is retrieved from source s and follows multinomial distribution: $w_{s,k} \sim \text{Multi}(\phi_{z_{s,k}})$.
- Q_i is the relevance score of each topic i and is sampled from a log-Normal distribution with mean 0.25 and standard deviation 1.5.
- m_k is the relevance score of each item k , which is derived as the weighted average across topic scores based on the item distribution over 8 latent topics, i.e., $m_k = \sum_{i=1}^T \phi_{i,k} Q_i$.
- c_s is the infrastructure cost per fetched item for source s . The cost c_s is assumed to be positively correlated with source relevance score $q_s = \sum_{i=1}^T \theta_{s,i} Q_i$ and follows a Gaussian distribution with mean $\frac{q_s}{2 \sum_{s=1}^S q_s}$ and standard deviation of 0.1.

To simulate the retrieval of one item from the source s , we sample a topic for an item k from the multinomial $\text{Multi}(\theta_s)$, i.e., $z_{s,k} \sim \text{Multi}(\theta_s)$, and sample an item $w_{s,k} \sim \text{Multi}(\phi_{z_{s,k}})$ where $w_{s,k}$ indicates item k being retrieved from source s . Given the sourcing policy $\mathbf{x} \in \mathbb{R}^S$, we execute the above sampling \mathbf{x}_s times for each source s as described at lines 1 in Algorithm 1, and then compute the quality score given a list of retrieved items.

The overall content relevance score is the sum of the content relevance scores after de-duplicating the retrieved content. The infrastructure load is a sum of products of a number of retrievals and the cost per fetched item c_s for each source, in which c_s varies across sources and positively correlates with the source relevance score. This setup is based on the real-world observation that sources providing higher relevance content are generally more computationally expensive. The objective in the benchmark experiments is a weighted sum of overall content relevance and negative infrastructure load. In the experiment, we repeat this simulation (at line 10) 1000 times for a given policy and compute the mean and standard error of the objective values, which we refer to as the *quality score* in the main text.

Algorithm 1 Recsys Simulation

```

1: procedure ITEM-RETRIEVAL( $x_s$ )
2:    $\vec{n}_s \leftarrow \vec{0} \in \mathbb{R}^K$  ▷ number of retrievals for  $K$  distinct items
3:   for  $n \leftarrow 1$  to  $x_s$  do ▷ retrieve  $x_s$  items
4:     Sample a topic for an item  $k$  in source  $s$  i.e.  $z_{s,k} \sim \text{Multi}(\theta_s)$ 
5:     Sample an item  $w_{s,k} \sim \text{Multi}(\phi_{z_{s,k}})$ 
6:      $\vec{n}_s \leftarrow \vec{n}_s + \vec{w}_s$ 
7:   end for
8:   return  $\vec{n}_s$ 
9: end procedure

10: procedure SOURCING( $\mathbf{x}$ )
11:   $\vec{n} \leftarrow \vec{0} \in \mathbb{R}^K$  ▷ number of retrievals for  $K$  distinct items
12:  for  $s \leftarrow 1$  to  $S$  do ▷ retrieve items for each source  $s$ 
13:     $\vec{n}_s \leftarrow \text{ITEM-RETRIEVAL}(x_s)$ 
14:     $\vec{n} \leftarrow \{\vec{n} + \vec{n}_s\}$ 
15:  end for
16:  Compute relevance score  $\text{RS} = \sum_{k=1}^K \mathbb{1}(n_k > 0)m_k$  and infrastructure cost  $C = \sum_{s=1}^S c_s \times x_s$ 
17:  return quality score  $Q = \text{RS} - 0.6 \times C$ 
18: end procedure

```

S2.2 SENSITIVITY ANALYSIS OF REGULARIZATION PARAMETER λ

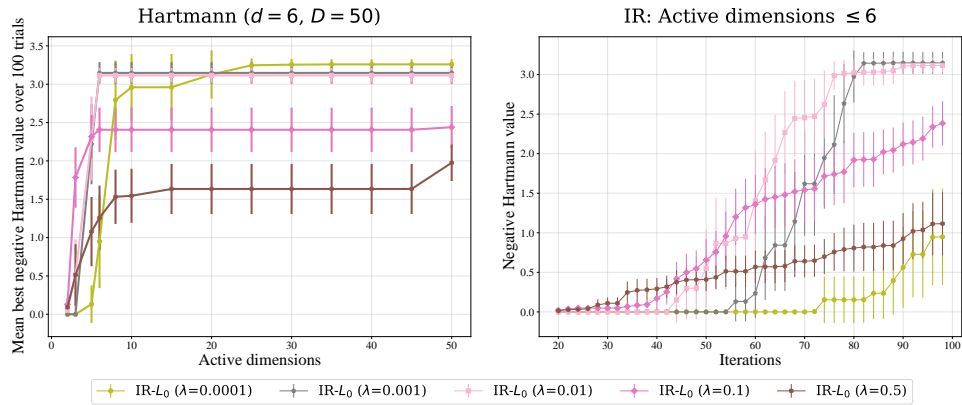


Figure S2: Results of EI-IR with different λ values for Hartmann6 function embedded into a 50D space. (Left) The objective-sparsity trade-off after all 100 iterations. (Right) The best objective function value considering only observations with at most 6 active (non-sparse) parameters.

We conduct a sensitivity analysis of regularization parameter λ used by IR and ER by sweeping different values of λ on the 50D Hartmann6 benchmark. The results are given in Fig. S2 and Fig. S3. We observe that we are able to control the sparsity level by appropriately choosing λ . In general, larger λ implies stronger regularization and results in finding configurations with a higher level of sparsity. When λ increases above a certain point, the regularization becomes too strong and fails to help find high-quality sparse points.

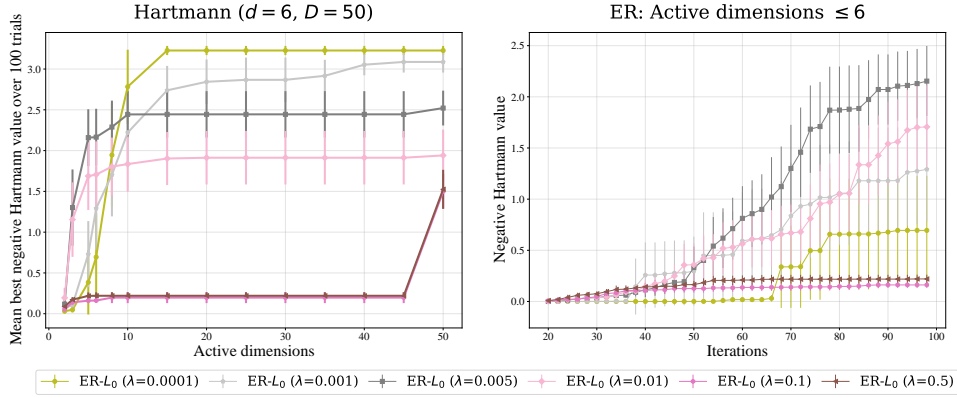


Figure S3: Results of EI-ER with different λ values for Hartmann6 function embedded into a 50D space. (Left) The objective-sparsity trade-off after all 100 iterations. (Right) The best objective function value considering only observations with at most 6 active (non-sparse) parameters.

By comparing results of IR and ER for different λ values, we note that IR is able to achieve effective optimization performance over a wider range of λ 's while ER is more sensitive to the value of λ . This validates the discussion about ER in Section 3.1 that ER is not as effective as IR due to ER's inability to select a new sparse point that improves over sparse points from previous iterates if the new sparse point does not improve on the dense points that are already observed.

S2.3 BENCHMARKS WITH L_1 REGULARIZATION

Our proposed method can work together with different forms of sparsity. Here we show the results of EI-ER, EI-IR and SEBO using L_0 regularization for the Hartmann6 function embedded in a 50D space. As can be seen in Fig. S4, using L_0 leads to significant improvement over L_1 for all three methods.

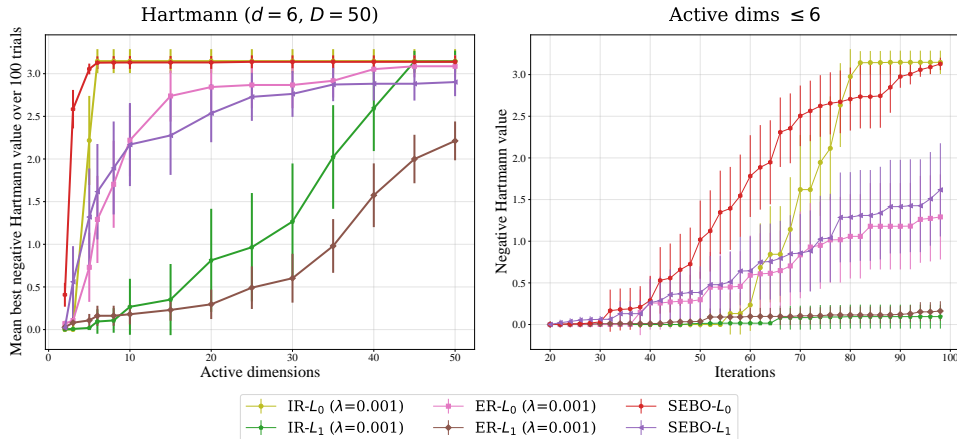


Figure S4: Results for the Hartmann6 function embedded in a 50D space. (Left) L_0 regularization outperforms L_1 regularization in exploring the objective-sparsity trade-offs for IR, ER and SEBO. (Right) L_0 regularization obtains better optimization performances considering only observations with at most 6 active (non-sparse) parameters.

S2.4 ABLATION STUDY ON USING SAAS

To illustrate the importance of using the SAAS model, we compare to using EI-IR- L_1 with a standard GP in Fig. S5. We observe that EI-IR- L_1 with a standard GP fails to discover non-trivial sparse configurations for all values of λ . This confirms that sparsity in the GP model is crucial for finding sparse configurations. This can also be observed by comparing performances of SAASBO and GPEI in Fig. 2 where there is a huge gap in terms of the best function value optimized even when looking at dense points (active dimensions = 50).

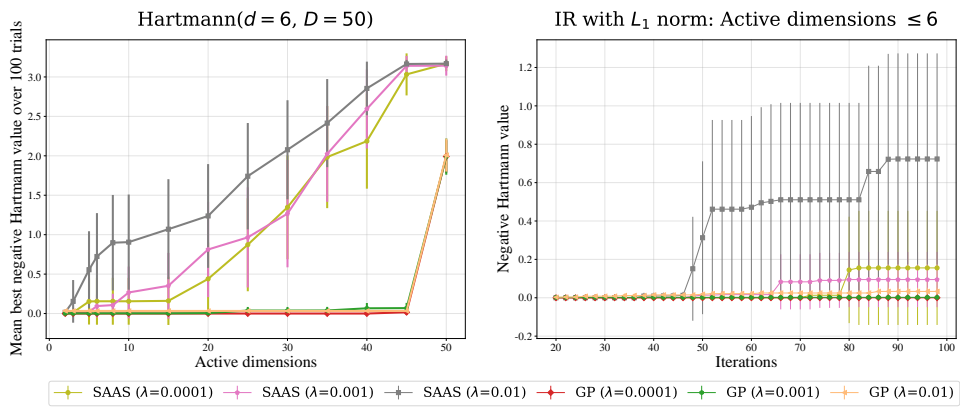


Figure S5: Results for the Hartmann6 function embedded in a 50D space. EI-IR- L_1 using the SAAS model significantly outperforms EI-IR- L_1 using a standard GP.